

# PROCESS-PARAMETER-DEPENDENT SPRING-IN AND WARPAGE OF LOCALLY REINFORCED UD TAPE LAMINATES AND V-SHAPED PROFILES

Benjamin Hangs<sup>1</sup>, Tobias Link<sup>1</sup> and Frank Henning<sup>1</sup>

<sup>1</sup>Polymer Engineering, Fraunhofer Institute for Chemical Technology (ICT),  
Joseph-von-Fraunhofer-Straße 7 in 76327 Pfinztal, Germany  
Email: benjamin.hangs@ict.fraunhofer.de, website: www.ict.fraunhofer.de

**Keywords:** tailored layup, spring-in, warpage, UD tape, thermoplastic composites

## Abstract

To take full advantage of the lightweight potential of thermoplastic advanced composites, a promising approach is the creation of tailored structures with locally reinforced, load bearing areas. However, especially in thin-walled structures this design strategy induces shape deformations due to the highly anisotropic material behavior of composites. In order to quantify these deviations, this paper presents a study on thin-walled tailored laminates made from thermoplastic unidirectional tape. Rectangular cross-ply layups were combined with a centered, longitudinal and unidirectional patch. The study covers the two relevant process stages of part manufacturing, which includes the consolidation of flat laminates and the subsequent forming of V-shaped profiles. To determine the influence of processing on the resulting spring-in and warpage, the forming pressure and mold temperature were varied on three levels. Based on characteristic geometric parameters, the results showed that tool temperature is the dominant influence, while forming pressure is of minor relevance. Furthermore, the underlying design of the experiments allowed the derivation of descriptive models to predict shape deformations with a high level of accuracy.

## 1. Introduction

Shape deformations and the corresponding residual stresses of continuous-fiber-reinforced composites are a severe issue in composite manufacturing that has been widely investigated since the 1980s [1-4]. Key drivers are the highly anisotropic in-plane and out-of-plane material properties and the resulting thermal strains and stresses in the cooling stage [5-8]. As a consequence, thermoplastic composites are even more prone to shape deformations than thermosets due to their higher processing temperatures. The challenge of undesirable shape deformations is greater if thin-walled, locally reinforced laminates are used to fully exploit the lightweight potential of advanced composites. As a result, such designs are not yet widely applied in industry. Instead, quasi-isotropic layups are predominantly used. This study seeks to bridge this gap by specifically focusing on thin-walled tailored layups made from thermoplastic unidirectional tape (UD tape). This material type enables the creation of laminates with any desired fiber orientation, stacking sequence and profiled wall thickness.

## 2. Study overview

The results presented below form part of a more extensive study on shape deformations of thin-walled, tailored thermoplastic laminates. The overall goal of that study is to develop a methodology to predict and evaluate such complex shape deformations numerically as well as experimentally. In total, fourteen layup variants are experimentally investigated in a two-stage manufacturing process as introduced below. Numerous characteristic parameters are derived from three-dimensional scan data to

quantitatively describe the coupons' complex and superimposing deformation modes. Out of this larger variety, one representative layup configuration is presented, which is additionally investigated with regard to varying process parameters. The warpage and spring-in of this layup variant are analyzed as an example, based on a two-stage design of experiments.

## 2.1. Coupon design and manufacturing

Locally reinforced consolidated laminates as well as 90° V-profiles are investigated to determine the influence of tailored layups on warpage and spring-in. Both coupons consist of a rectangular  $(0_2, 90_2)_s$  baseplate G onto which a unidirectional  $(0)_8$  patch-reinforcement P is positioned, centered in longitudinal direction. Figure 1 illustrates the coupons and relevant dimensions. The difference in patch width is a result of transversal squeeze flow in this section. The coupons are made from carbon-fiber-reinforced unidirectional tape (UD tape) with a polyphenylene sulfide matrix (CF/PPS) which was provided by Celanese. This thermoplastic semi-finished product contains 53 % fibers by volume and is specified with a single-ply thickness of 0.16 mm.

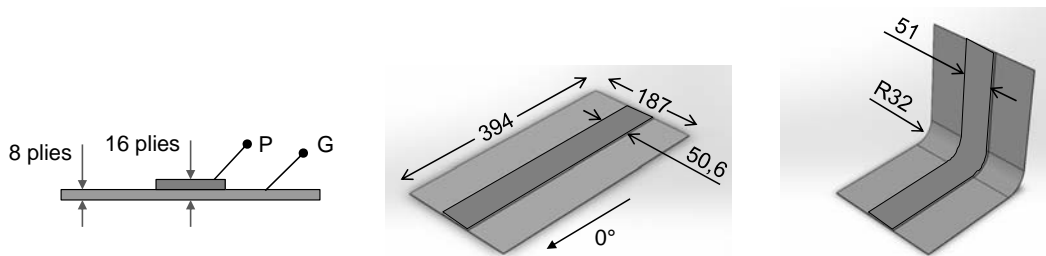


**Figure 1.** Coupon design and dimensions

In an initial step, the UD tape is processed using automated Relay 2000 tape-placement technology to create spot-welded tape layups. Further details of this tape-laying process are provided in [9]. The subsequent coupon manufacturing is subdivided into two steps. Process stage 1 (PS1) is consolidation of the spot-welded tape layups to create monolithic laminates. This is realized in the HTP process (Heating - Transfer - Pressing), which is illustrated in Figure 2. To heat up the material to processing temperature ( $T_{h,PS1} = 305 \text{ }^\circ\text{C}$ ), two tape layups at a time are placed between two pieces of aluminum sheet metal. Grooves are milled into the lower sheet metal to fit the local patch reinforcement. Afterwards this stack is placed into a temperature-controlled contact heating device. Once the processing temperature is reached, the stack is transferred quickly into a flat shear edge mold and then rapidly cooled down under pressure for 60 seconds.

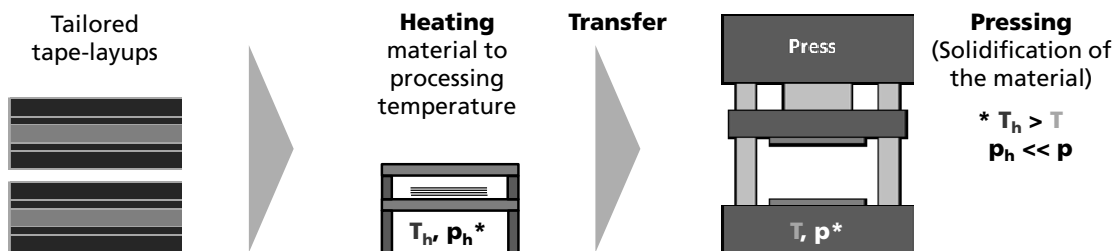


**Figure 2.** Schematic of process stage 1 - consolidation of tailored tape layups

Process stage 2 (PS2) describes the forming of the consolidated tailored laminates to create the 90° V-profiles. Again, an HTP approach is used, in which the coupons are heated in a convection oven. A

single V-shaped aluminum sheet metal serves as a carrier to support the softening laminate. While softening, the material bends due to gravity, and as a result the laminate clings to the sheet metal carrier. Forming is therefore finished at the end of the heating cycle (processing temperature  $T_{h,PS2} = 340\text{ }^{\circ}\text{C}$ ). After transferring the material into the hydraulic press, a matched metal mold is used for solidification.

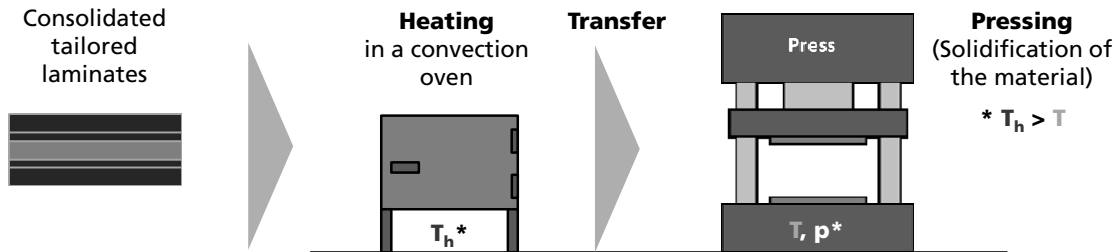


**Figure 3.** Schematic diagram of process stage 2 - forming of V-profiles

## 2.2. Experimental design

In order to investigate the interaction of process parameters and resulting shape deformations of tailored laminates, forming pressure  $p$  and tool temperature  $T$  are considered. Both factors are varied on three levels which are summarized in Table 1. Individual parameter combinations are written as for example p1T1, p2T3, etc. A two-stage design of experiments is applied to cover PS1 as well as PS2. This includes a full factorial variation for PS1, followed by a linear D-optimal test plan for PS2.

**Table 1.** Definition of process parameter levels

Forming pressure $p$ in MPa			Tool temperature $T$ in $^{\circ}\text{C}$		
p1	p2	p3	T1	T2	T3
1	3	5	100	150	200

## 2.3. Characterization of shape deformations

To accurately determine the shape of the deformed coupon, a hand-operated FaroArm with an integrated Descam ModelMaker Z laser scanner is used to generate three-dimensional point clouds of the coupon surface. During the scanning procedure, the coupons are positioned in a jig to ensure high repeatability. Based on an automated alignment of scan data and ideal geometry, it is possible to derive characteristic parameters which enable the shape deformations of the coupon to be quantified.

Figure 4 illustrates the characteristic parameters which are used in this article to evaluate warpage in PS1 and PS2. The first warpage-parameter  $h_{KS}$  is determined by the average maximum vertical deflection of the data points at the extreme left and right. In addition,  $\Omega_{KS} = \kappa_{KS} / \alpha_{KS}$  represents the cross section form factor of a coupon.  $\kappa_{KS}$  is the patch curvature and  $\alpha_{KS}$  is the enclosed angle of the left and right baseplate sections. The values of  $h_{KS}$  and  $\Omega_{KS}$  are determined at three positions along the coupon ( $h_{KSL}$ ,  $h_{KSM}$  and  $h_{KSR}$ ) to evaluate a potential change in cross section. Furthermore, Figure 4 shows the definition of spring-in  $\theta = \beta - \beta_0$  in PS2, the angular change of the V-profiles.

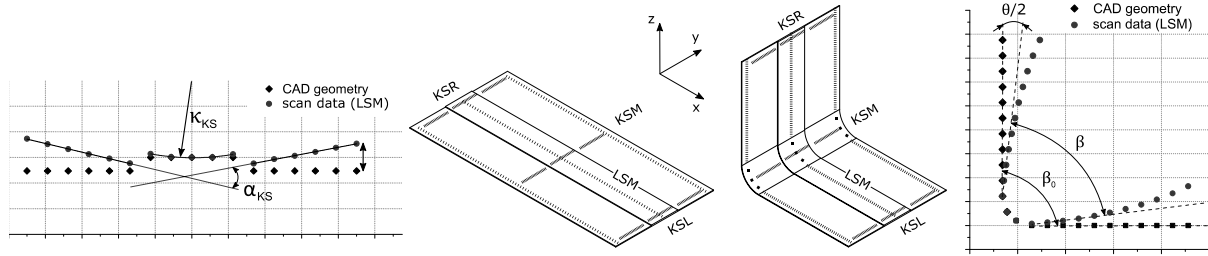


**Figure 4.** Illustration of the derived characteristic parameters to quantify shape deformations

### 3. Results and discussion

The results presented below are based on a minimum of three samples per process parameter combination. In cases of increased result variance, a higher number of coupons was produced and analyzed to increase the statistical validity of the data. Outliers within the results were identified with box plots. The chosen criterion is a 1.5-times interquartile range.

#### 3.1. Process stage 1: consolidated laminates

Figure 5 illustrates  $h_{KS}$  as a function of process parameter combinations. The data is sorted by tool temperature  $T$  to generate an overview of lateral warpage in consolidated tailored laminates. The data reveals a heterogeneous impression with an increased level of deflection for  $h_{KSM,T2}$  and  $h_{KSL,T2}$  compared to the  $T1$  and  $T3$  variants. The values of  $h_{KSR}$ , on the other hand, show a trend towards reduced deflections and increased variance compared to  $h_{KSL}$  and  $h_{KSM}$ . Correlation of physical coupons and scan data revealed that this effect is caused by blocked squeeze flow at the tool's shear edge next to  $h_{KSR}$ . As a result, a burr is created, causing edge stiffening. By cooling the material below its glass transition temperature, this state is "frozen", resulting in the observed deviation of  $h_{KSR}$  from  $h_{KSL}$  and  $h_{KSM}$ . The experimental design nevertheless revealed a clear quadratic dependency between  $h_{KS}$  and  $T$ , see Figure 6. The model fit is, however, lower for  $h_{KSR}$ . A correlation of  $h_{KS}$  and forming pressure  $p$  was not identified.

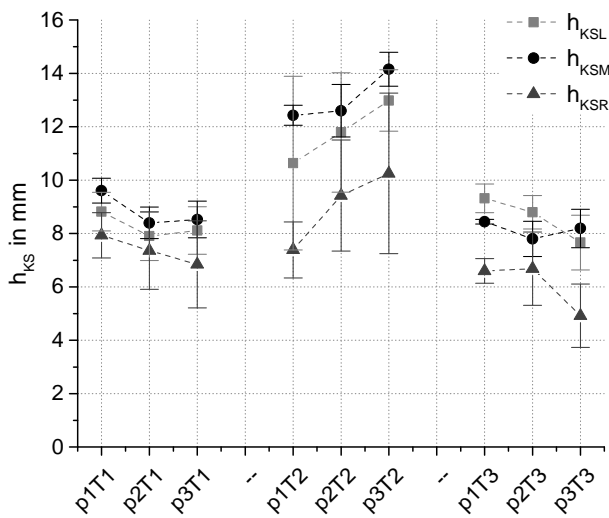


**Figure 5.** Lateral warpage  $h_{KS}$  in PS1, sorted by tool temperature  $T$

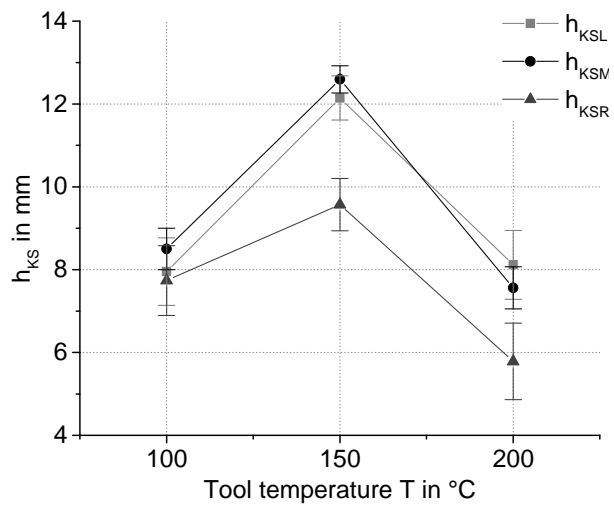


**Figure 6.** Main effect plot of  $h_{KS}$  vs.  $T$  (95% confidence level)

The effect for reduced  $h_{KSR}$  values in PS1 is also apparent with regard to the coupons' form factor  $\Omega_{KS}$ , as shown in Figure 7. The graph firstly reveals a clear reduction of the absolute  $\Omega_{KS}$  values for tool temperature  $T3$ . In addition,  $\Omega_{KSL}$  and  $\Omega_{KSR}$  seem to show a slight sensitivity of the mean  $\Omega$ -values when the forming pressure  $p$  is increased. This assumption is verified by further analysis of the data as part of the statistical experimental design. The identified dependence of  $\Omega_{KS}$  on the process parameters  $T$  and  $p$  is illustrated in Figure 8.

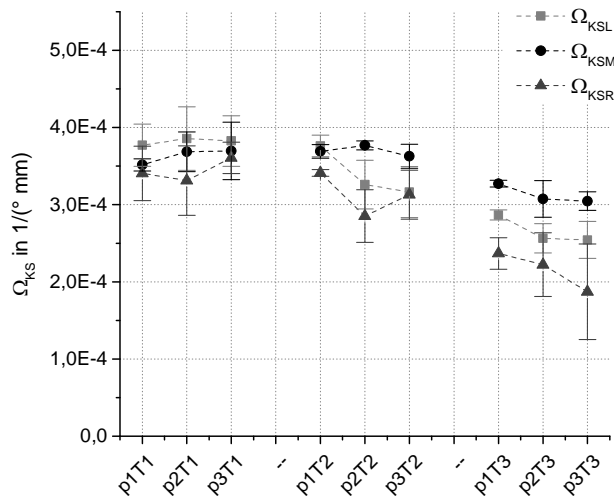


Figure 7. Form factor  $\Omega_{KS}$  in PS1, sorted by tool temperature  $T$

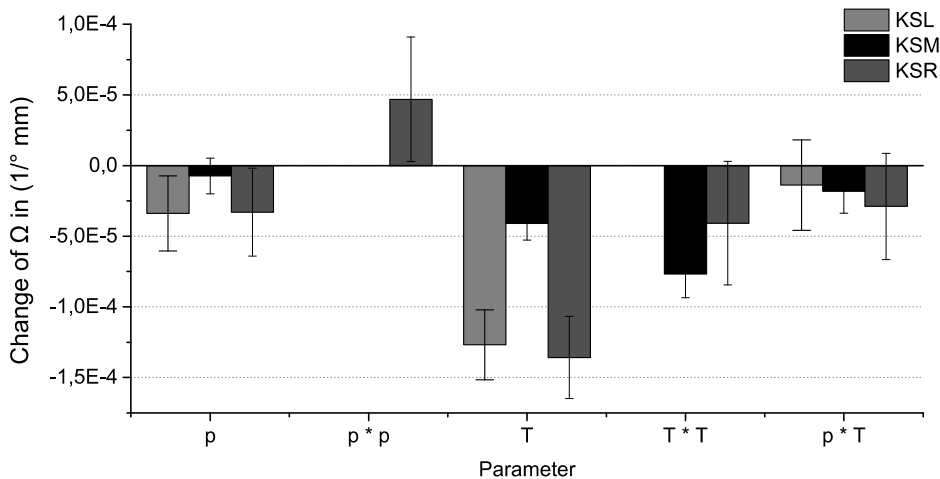
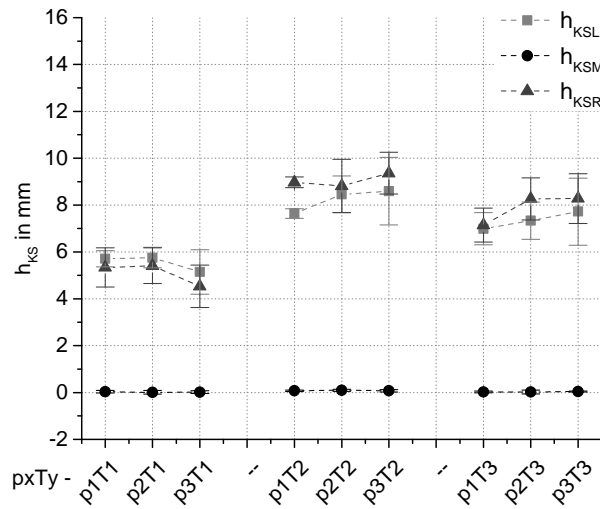


Figure 8. Influence of  $T$  and  $p$  on the form factor  $\Omega_{KS}$  in PS1, determined by experimental design

### 3.1. Process stage 2: V-profiles

Contrary to PS1, the PS2 scan data shows significantly reduced variance of the  $h_{KSR}$  values, and absolute values are harmonized with  $h_{KSL}$  (Figure 9). This supports the above mentioned theory of edge stiffening caused by blocked squeeze flow. By heating the material above the melting temperature, the deformations are relieved and, since V-profiles are manufactured by matched-metal molding, no unsymmetrical burr is created for  $h_{KSL}$  and  $h_{KSR}$ , so that the warping of the coupons

happens unimpeded. The predictive quality of the model, derived from the experimental design and shown in Figure 10, is accordingly high.



**Figure 9.** Lateral warpage  $h_{KS}$  in PS2, sorted by tool temperature  $T$

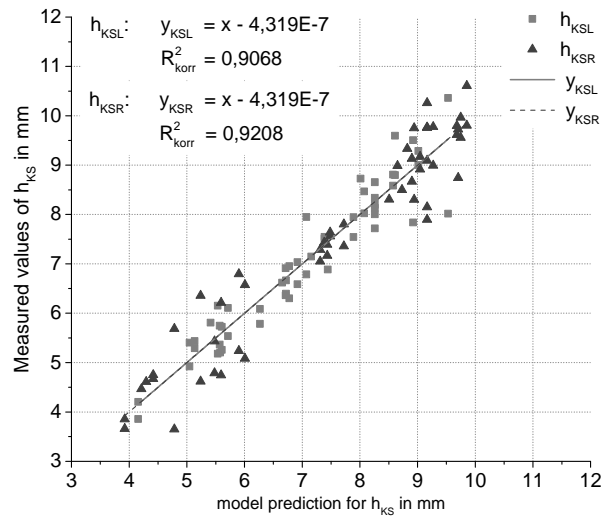


**Figure 10.** Comparison of scan data and predictive model for  $h_{KS}$  in PS2

A direct comparison of  $\Omega_{KS,PS2}$  with PS1-data shows good correlation of the form factor for  $T1$ . Contrary to this observation, a significant increase of  $\Omega_{KS}$  is observed for the  $T2$  and  $T3$  variants. At the same time, the maximum difference in the mean values  $|\Omega_{KSL} - \Omega_{KSR}|$  is reduced by a factor of 3.66 for PS2 in comparison to PS1. Once again, these effects can be described by a statistical model, which is shown in Figure 12. The predictive quality for  $\Omega_{KSR}$  is reduced compared to  $\Omega_{KSL}$  and  $h_{KS}$ , though. This may partly be caused by the remaining effects of blocked squeeze flow in PS1, which cannot be fully recovered by the reheating to processing temperature in PS2.

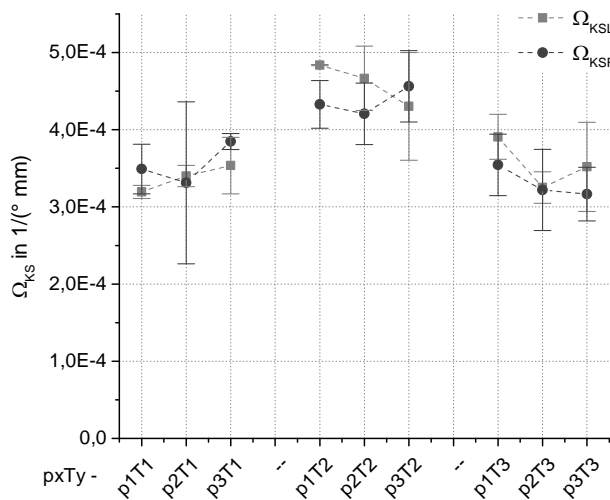


**Figure 11.** Form factor  $\Omega_{KS}$  in PS2, sorted by tool temperature  $T$

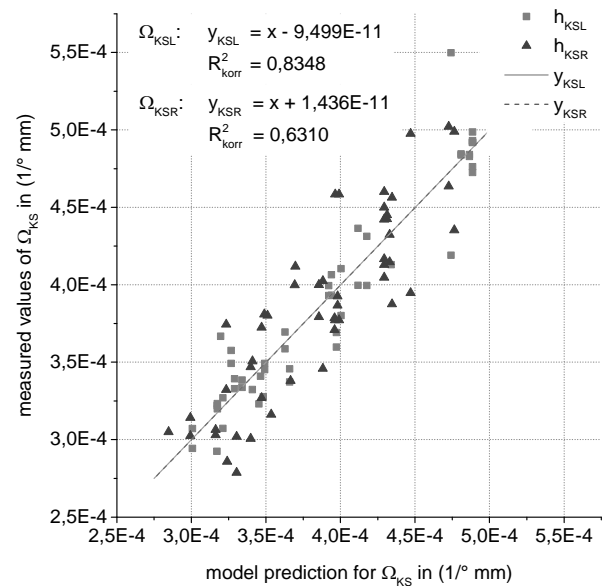


**Figure 12.** Comparison of scan data and predictive model for  $\Omega_{KS}$  in PS2

Concluding this characterization of shape deformations, Figure 13 shows spring-in  $\theta$  of 90° V-profiles as a function of process parameter combinations. The spectrum of mean values ranges from -0.07° (p2T3) to 1.35° (p3T1). Again, the dominant influence of tool temperature  $T$  is apparent. Positive  $\theta$  values correspond here with enclosed angles larger than 90° and hence a widening of the V-profiles. This enclosed angle is, in approximation, linearly reduced with increasing tool temperature, which corresponds to lower  $\theta$  values. This behavior is in agreement with the predominant opinion in literature. The observed positive spring-in values are partially related to the superposed lateral warpage and the fact that the spring-in angle is determined at the longitudinal median plane of the coupon. Despite this superposition of shape deformations, spring-in  $\theta$  can be predicted with high accuracy based on the predictive model shown in Figure 14.

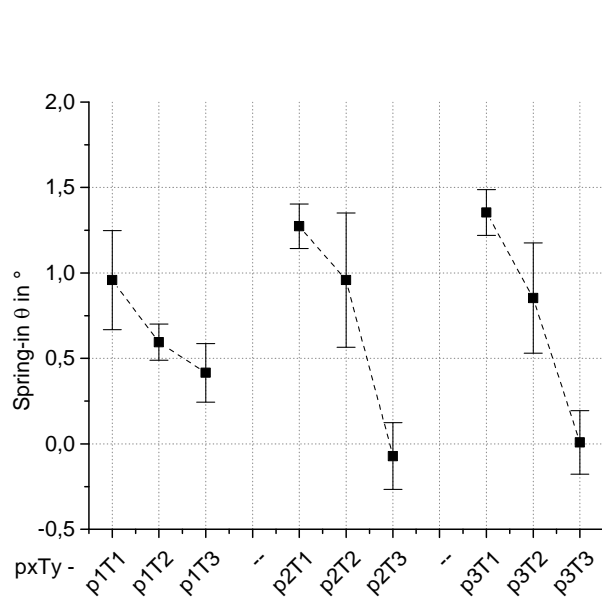


**Figure 13.** Spring-in  $\theta$  of V-profiles in PS2, sorted by forming pressure  $p$

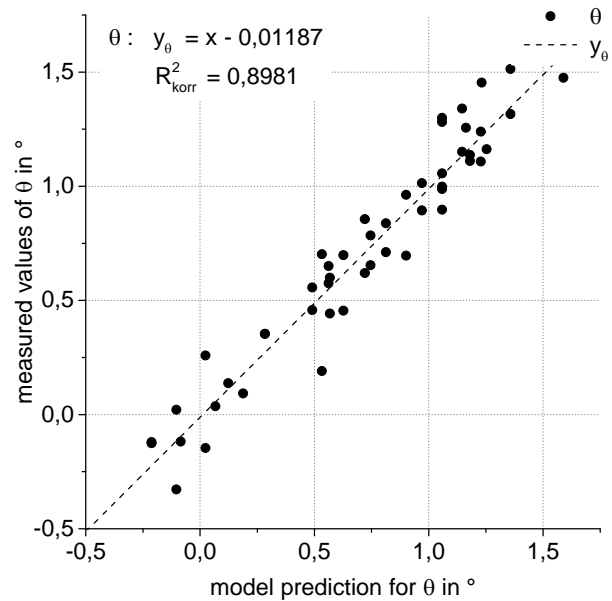


**Figure 14.** Comparison of scan data and predictive model for  $\theta$  in PS2

#### 4. Conclusion

An experimental investigation was presented, which focused on process- and layup-induced shape deformations of thin-walled, locally reinforced tailored laminates made from CF/PPS UD tape. Forming pressure and tool temperature were varied on three levels. A two-stage design of experiments was applied, covering the laminate consolidation (PS1) and subsequent forming of V-profiles (PS2). Laser scanning was then used to generate three-dimensional point clouds of the manufactured coupons. Based on the generated scan data, characteristic parameters were derived to comprehensively evaluate the warpage and spring-in of the coupons. The results revealed a dominating influence of tool temperature, whereas forming pressure was of minor relevance. The experimental design furthermore allowed the generation of descriptive models to predict shape deformations with high accuracy.

#### Acknowledgments

This work was funded by the Fraunhofer-Gesellschaft as part of the MEF project *SpannEnd*. The authors furthermore gratefully acknowledge the support of their colleagues at Fraunhofer IWM, who provided the laser scanner.

## References

- [1] S. Pagliuso. Warpage, a nightmare for composite part producers. *Progress in Science and Engineering of Composites*, 1617-1623, 1982
- [2] D.W. Radford and R.J. Diefendorf. Shape instabilities in composites resulting from laminate anisotropy. *Journal of Reinforced Plastics and Composites*, 12(1): 58-75, 1993
- [3] G. Fernlund et al. Experimental and numerical study of the effect of cure cycle, tool surface, geometry and lay-up on the dimensional fidelity of autoclave-processes composite parts. *Composites Part A: Applied Science and Manufacturing*, 33(3): 341-351, 2002
- [4] E. Kappel, D. Stefaniak and G. Fernlund. Predicting process-induced distortions in composite manufacturing – A pheno-numerical simulation strategy. *Composite Structures*, 120: 98-106, 2015
- [5] J. A. Nairn and P. Zoller. Matrix solidification and the resulting residual thermal stresses in composites. *Journal of Material Science*, 20(1): 355-367, 1985
- [6] J. A. Nairn and P. Zoller. The development of residual thermal stresses in amorphous and semicrystalline thermoplastic matrix composites. *Toughened Composites*, STP937: 328-341, 1987
- [7] W.E. Lawrence, J.-A. Manson and J.C. Seferis. Thermal and morphological skin-core effects in processing of thermoplastic composites. *Composites*, 21(6): 475-480, 1990
- [8] P. Parlevliet, H.E.N. Bersee and A. Beukers. Residual Stresses in thermoplastic composites – A study of the literature – Part I. *Composites Part A: Applied Science and Manufacturing*, 31(11): 1847-1857, 2006
- [9] B. Hangs, F. Henning, M. Knoch and T. Huber. Evaluation of process- and layup-induced warpage of tailored PPS/CF laminate. *Proceedings of the SPE Automotive Composites Conference & Exhibition (ACCE), Novi, USA, September 09-11 2014.*